Separation Science and Technology
Publication details, including instructions for authors and subscription information:
http://www.informaworld.com/smpp/title~content=t713708471

Determination of Microbial Sorption Isotherms from Column Experiments

Junliang Liu[a]; Mingqi Qiao[b]; Huiyun Zhang[c]; Wenfu Yang[d]; Gang Chen[e]
[a] College of Urban Construction, Hebei Agricultural University, Baoding, Hebei, the P. R. China [b] College of Traditional Chinese Medicine Basic Theory, Shandong University of Traditional Chinese Medicine, Jinan, the P. R. China [c] Scientific Research Office, Shandong University of Traditional Chinese Medicine, Jinan, the P. R. China [d] Jiaozhou People's Hospital, Jiaozhou, the P. R. China [e] Department of Civil and Environmental Engineering, FAMU-FSU College of Engineering, Tallahassee, Florida, USA

To cite this Article Liu, Junliang , Qiao, Mingqi , Zhang, Huiyun , Yang, Wenfu and Chen, Gang(2006) 'Determination of Microbial Sorption Isotherms from Column Experiments', Separation Science and Technology, 41: 16, 3639 — 3654
To link to this Article: DOI: 10.1080/01496390600957116
URL: http://dx.doi.org/10.1080/01496390600957116

Separation Science and Technology, 41: 3639–3654, 2006

ISSN 0149-6395 print/1520-5754 online
DOI: 10.1080/01496390600957116

Determination of Microbial Sorption Isotherms from Column Experiments

Junliang Liu
College of Urban Construction, Hebei Agricultural University, Baoding, Hebei, the P. R. China

Mingqi Qiao
College of Traditional Chinese Medicine Basic Theory, Shandong University of Traditional Chinese Medicine, Jinan, the P. R. China

Huiyun Zhang
Scientific Research Office, Shandong University of Traditional Chinese Medicine, Jinan, the P. R. China

Wenfu Yang
Jiaozhou People's Hospital, Jiaozhou, the P. R. China

Gang Chen
Department of Civil and Environmental Engineering, FAMU-FSU College of Engineering, Tallahassee, Florida, USA

Abstract: Microbial sorption isotherms cannot be obtained using the traditional batch methods owing to the difficulty of distinguishing between reversible and irreversible sorption. In this research, we investigated microbial sorption isotherms of *Pseudomonas fluorescens, Pseudomonas putida*, and *Pseudomonas* sp. on an alluvial loam from the Central Oklahoma Aquifer (COA) using column experiments. All these three bacterial strains displayed a concave isotherm on COA, which can be described by the Freundlich sorption isotherms. We explained the concave-shaped microbial sorption isotherms using the surface thermodynamic theory. In this study, we also investigated

Received 30 March 2006, Accepted 2 August 2006
Address correspondence to Gang Chen, Department of Civil and Environmental Engineering, FAMU-FSU College of Engineering, 2525 Pottsdamer Street, Tallahassee, FL 32310, USA. Tel.: (850) 4106303; Fax: (850) 4106142; E-mail: gchen@eng.fsu.edu

the impact of transport velocity on the microbial breakthrough curves. We found that the same bacterial strain had the same sorption isotherms but different deposition coefficient at different flow rates. The high solid to solution ratio of column experiments is close to that which is encountered in the natural systems, which makes this method a useful tool for guidance of *in-situ* bioremediation.

Keywords: Sorption isotherm, column experiment, *Pseudomonas fluorescens*, *Pseudomonas putida* and *Pseudomonas* sp.

INTRODUCTION

Interest in predicting the fate and transport of microbes in the subsurface is motivated by either a concern that microbes can contaminate drinking water supplies or their role in bioremediation (1). Microbial transport is greatly impacted by their irreversible deposition (2–8) and reversible sorption (9–14) on the media matrices. The movement and spreading of microbes during transport can be described by a combined model that incorporates the Deep-Bed Filtration Model into a simple Convection-Dispersion Model (ignoring biodegradation) (6, 15):

$$\theta\frac{\partial C}{\partial t} + (1-\theta)\rho_b\frac{dS}{dt} = D\theta\frac{\partial^2 C}{\partial x^2} - v\theta\frac{\partial C}{\partial x} - \theta k_c C \tag{1}$$

where θ is the porosity (m^3/m^3); C microbial concentration in solution (number of cells/m^3); t elapsed time from the initial microbial injection (sec); ρ_b sediment bulk density (g/m^3); S concentration of reversibly adsorbed microbes on the porous medium (cells/g); D hydrodynamic dispersion coefficient (m^2/sec); v interstitial pore water velocity (m/sec); x longitudinal coordinate (m); and k_c deposition coefficient that indicates the rate of irreversible adsorption of microbes on the porous medium (sec^{-1}). Using this model, Harvey and Garabedian (6) observed a good fit of model simulations to breakthrough curves (BTCs) for concentrations of both bromide and bacteria in effluent from sand columns.

The reversible sorption of bacteria onto the porous medium can be expressed in term of solution concentration (16):

$$\frac{dS}{dt} = \frac{\partial S}{\partial C}\frac{\partial C}{\partial t} \tag{2}$$

By substituting equation (2) into equation (1) and rearranging, a one-dimension transport can be expressed as:

$$\left(1 + \frac{1-\theta}{\theta}\rho_b\frac{dS}{dC}\right)\frac{\partial C}{\partial t} = D\frac{\partial^2 C}{\partial x^2} - v\frac{\partial C}{\partial x} - k_c C \tag{3}$$

where $(1 + 1 - \theta/\theta)\rho_b$ (dS/dC) is defined as retardation factor, R, which is the average transport velocity of bacteria (v_{av}) relative to that of water (v_w),

such that $R = v_{av}/v_w$. The reversible microbial sorption on the porous medium is determined by their sorption isotherms. Due to the difficulty of distinguishing between reversible and irreversible sorption, microbial sorption isotherms cannot be achieved in batch experiments. Column experiments for the determination of sorption parameters, which borrows the idea from nonlinear chromatography, have been developed (11).

In the case of linear adsorption isotherms, such that $(dS/dC) = K_p$, where K_p is the microbial distribution coefficient between the aqueous phase and the porous media (m^3/g), R will be a constant and independent of microbial solution concentration. Accordingly, equation (3) can be easily solved and used to fit the microbial transport BTCs. While for nonlinear isotherms, R will depend on the microbial solution concentration and equation (3) will be a non-linear differential equation and can only be solved using numerical methods.

The objectives of this study were to characterize microbial sorption isotherms on an alluvial loam from Central Oklahoma Aquifer (COA) using column experiments. The validity of the isotherms was established by fitting the microbial transport BTCs using numerical methods. We investigated the interfacial interaction free energy between microbes and media matrices and explained the sorption isotherms using the thermodynamic theory.

MATERIALS AND METHODS

Bacterial Strains and Growth Conditions

Three bacteria, *Pseudomonas fluorescens, Pseudomonas putida*, and *Pseudomonas* sp. were selected for this study, which were typical representatives of microorganisms used in bioremediation of contaminated soil and associated groundwater. They were all obtained from ATCC (17559, 12633, and 55648) and grown on Nutrient Broth (Difco 0003) at 26°C, 26°C, and 30°C, respectively until reaching a stationary state. Before the column experiments, the bacterial strains were centrifuged at 2500 RPM (Damon/IEC Divison, Needham Heights, MA) and washed twice with a sterilized buffer solution (potassium phosphate monobasic-sodium hydroxide buffer, Fisher Scitific, Pittsburgh, PA). They were and then resuspended in sterilized nano-pure deionized water (NPDI, Barnstead, Dubuque, IA) to make a bacterial solution. After the washing process, the soluble exopolysaccharide (if any) was stripped off the bacteria (17). During transport in the column, the growth of the bacteria was assumed to be minimal due to the lack of substrate or nutrient and short retention time. Therefore, the bacterial surface property should remain unchanged during transport and could be described by their surface thermodynamics. Bacterial concentrations were quantified by Adenosine Triphosphate (ATP) analysis (15).

Porous Media

The porous media used in this research was an alluvial loam from the Central Oklahoma Aquifer (COA) (Norman, Oklahoma). The median grain radius size of COA was 65 μm with 38% passing a 200 sieve. The organic fraction and hydraulic conductivity were reported to be 0.340 ± 0.20 and $(8.2 \pm 1.3) \times 10^{-5}$ cm/s (18). Due to concerns about structural and chemical alterations, COA was not sterilized. Instead, it was air dried and stored and desiccated to minimize the presence of an active bacterial population.

Physiological State Determination

The stationary state of the bacteria was quantified through biochemical assay using ATP analysis (15). After inoculation, the cultures were placed on the Gyrotory Water Bath Shaker (New Brunswick Scientific Co. Inc. Model G76) at 150 RPM. 50 μl of cultures was sampled at a time interval of 30 minutes. The light emission produced by the reaction of ATP extracted from the cells with luciferase as measured by a luminometer (TD-20/20, Turner Design, Sunnyvale, CA) was compared to an ATP standard (2.5×10^{-8} g/ml ATP which is equivalent to 5×10^7 bacteria per ml, 10 μg/ml ATP in HEPES buffer, Turner Design, Sunnyvale, CA) to determine the number of viable bacterial cells. In this way, curves of the number of viable bacterial cells versus time were obtained, which were used as the reference for the determination of the stationary state for different bacterial strains.

Measurement of Surface Thermodynamics

Surface thermodynamics of the media, COA, was studied using the wicking method (19, 20). This method determined the contact angle ($\cos\beta$) by measuring the velocity of capillary rise through a porous layer based on the Washburn equation:

$$h^2 = (R_e \cdot t \cdot \gamma_L \cdot \cos\beta) \cdot (2 \cdot \mu)^{-1} \quad (4)$$

where h is the height (m) of capillary rise of the wicking liquid at time t (sec); γ_L total surface tension of the wicking liquid (mJ/m^2); μ viscosity of the wicking liquid ($N \cdot s/m^2$) and R_e average interstitial pore size (m). By using a liquid with low surface tension, such as methanol ($\gamma = 22.5$ mJ/m^2) or hexane ($\gamma = 18.4$ mJ/m^2), the average interstitial pore size R_e can be obtained from equation (4) since methanol or hexane is expected to spread over the solid surface during the wicking measurement resulting in $\cos\beta = 1$. Once R_e was determined, an apolar liquid, diiodomethane and two polar liquids, glycerol and water were applied to estimate their respective $\cos\beta$ values.

Microbial surface thermodynamic properties were estimated by the contact angle measurement (Contact Angle Meter, Tantec, Schaumburg, IL) following the method described by Grasso et al. (21). Bacterial strains collected in the stationary state (predetermined by ATP analysis) were vacuum filtered on silver metal membrane filters (0.45 μm, Osmonic, Inc., Livermore, CA) and air-dried for about 30 minutes before the contact angle measurement. The amount of cells on the silver filter was approximately 13 mg to ensure a multi-layer covering of the membrane, and the moisture content was kept in the range of 25% to 30%. As described previously for the wicking method, diiodomethane, glycerol, and water were used for the contact angle measurement.

Each measurement was repeated 30 times and the surface thermodynamic parameters were estimated by Young-Dupré equation (5) using the average results.

$$(1+\cos\beta)\gamma_L = 2\left(\sqrt{\gamma_S^{LW}\gamma_L^{LW}} + \sqrt{\gamma_S^{+}\gamma_L^{-}} + \sqrt{\gamma_S^{-}\gamma_L^{+}}\right) \tag{5}$$

where γ_L is the surface tension of the liquid that is used for the measurement (mJ/m^2) which can be calculated by:

$$\gamma_L = \gamma_L^{LW} + 2\sqrt{\gamma_L^{-}\gamma_L^{+}} \tag{6}$$

where γ^{LW} is the Liftshitz-van der Waals component of surface tension (subscript S for solid and L for liquid) (mJ/m^2); γ^{+} electron-acceptor parameter and γ^{-} electron-donor parameter of the Lewis acid/base component of surface tension (subscript S for solid and L for liquid) (mJ/m^2).

Surface Thermodynamic Model Development

The Lifshitz-van der Waals and Lewis acid-base interactions between microbes 1 and medium matrix 2, immersed in water 3 were then estimated by equation (7) and (8) (22):

$$\Delta G(y)_{132}^{LW} = 2\pi R\frac{y_0^2}{y}\Delta G_{y_0 132}^{LW} \tag{7}$$

$$\Delta G(y)_{132}^{AB} = 2\pi R y_0 e^{(y_0-y)/\lambda}\Delta G_{y_0 132}^{AB} \tag{8}$$

where λ is the decay length of water, assumed to be 0.6 nm for pure water (23); y distance between the microbes (sphere) and the media matrices (flat plate) measured from the outer edge of the sphere (m); y_0 equilibrium distance that is assumed to be 1.57 Å by van Oss (23); R radius of the microbes (m); ΔG_{y0132}^{LW} and ΔG_{y0132}^{AB} Gibbs energies of two parallel plates, 1 and 2,

immersed in water 3 at the distance of y_0, which can be obtained from equations (9) and (10) (22):

$$\Delta G^{LW}_{y_0132} = -2\left(\sqrt{\gamma_3^{LW}} - \sqrt{\gamma_2^{LW}}\right)\left(\sqrt{\gamma_3^{LW}} - \sqrt{\gamma_1^{LW}}\right) \tag{9}$$

$$\begin{aligned}\Delta G^{AB}_{y_0132} = {} & 2\sqrt{\gamma_3^+}\left(\sqrt{\gamma_1^-} + \sqrt{\gamma_2^-} - \sqrt{\gamma_3^-}\right) \\ & + 2\sqrt{\gamma_3^-}\left(\sqrt{\gamma_1^+} + \sqrt{\gamma_2^+} - \sqrt{\gamma_3^+}\right) \\ & - 2\sqrt{\gamma_1^+\gamma_2^-} - 2\sqrt{\gamma_1^-\gamma_2^+}\end{aligned} \tag{10}$$

In equations (7) and (8), the microbes are modeled as a sphere having a radius at least one order of magnitude less than that of the media matrices. Therefore, a sphere-flat plate interaction is adopted to simplify the interactions between microorganisms and the media matrices.

When the media surface is occupied by deposited bacterial cells, the interactions between bacterial cells in solution and deposited cells on the medium surface will impact the interactions between the microbes in solution and the media matrices:

$$\Delta G(y)^{LW}_{131} = \pi R \frac{y_0^2}{y} \Delta G^{LW}_{y_0131} \tag{11}$$

$$\Delta G(y)^{AB}_{131} = \pi R y_0 e^{(y_0 - y)/\lambda} \Delta G^{AB}_{y_0131} \tag{12}$$

where ΔG^{LW}_{y0131} and ΔG^{AB}_{y0131} are Gibbs energy of interactions between sphere microbes 1, immersed in water 3 at the distance of y_0 and can be calculated using equations (9) and (10) by substituting 1 for 2.

The electrostatic interaction free energy, ΔG^{EL}_{131} and ΔG^{EL}_{132} can be evaluated by (constant potential approach) (valid for $0.1 < \kappa y < 300$, van Oss (23)):

$$\Delta G(y)^{EL}_{131} = 0.5 \cdot \pi\varepsilon\varepsilon_0 R\psi_{01}{}^2 \mathrm{Ln}(1 + e^{-\kappa y})] \tag{13}$$

$$\Delta G(y)^{EL}_{132} = \pi\varepsilon\varepsilon_0 R\psi_{01}\psi_{02} \mathrm{Ln}(1 + e^{-\kappa y})] \tag{14}$$

where ε and ε_0 are the relative dielectric permittivity of water (78.55 for water at 25°C) and permittivity under vaccum (8.854×10^{-12} C/V · m) respectively; ψ_{01}, ψ_{02} potentials at the surfaces of the microbes and the medium matrix; $1/\kappa$ Debye-Hückel length and also an estimation of the effective thickness of the electrical double layer (24). ψ_{01}, ψ_{02} can be calculated based on the following equation:

$$\psi_0 = \zeta(1 + z/a)\exp(\kappa z) \tag{15}$$

where ζ is the zeta potential measured at the slipping plate; z distance from the particle surface to the slipping plate that is generally on the order of 5 Å (23);

and *a* radius of the particle; ζ-potentials of the bacteria and the medium were measured by suspending in a 10^{-5} M NaCl solution using Lazer Zee Meter (Model 501, Pen Kem, Inc.).

Bacterial Transport Parameter Determination

The deposition coefficient k_c that describes the microbial irreversible sorption in porous media can be measured using equation (16) (2):

$$k_c = \frac{v}{L}\{-\mathrm{Ln}(fr) + \frac{[\mathrm{Ln}(fr)]^2}{Pe}\} \tag{16}$$

where L is the length between the injection and where the bacteria are collected or packed bed column length (m); *fr* microbial fraction recovery; *Pe* Peclet number, which can be obtained from studying the BTCs of a conservative tracer based on equation (17) (25, 26):

$$\sigma^2 = \tau^2 \cdot \left[\frac{2}{Pe} - \frac{2}{Pe^2} \cdot (1 - e^{-Pe})\right] \tag{17}$$

where σ is the standard deviation and τ measured average residence time for the tracer in the reactor (sec), determined by:

$$\tau = \frac{\int_0^\infty t \cdot C(t)dt}{\int_0^\infty C(t)dt} \tag{18}$$

$$\sigma^2 = \frac{\int_0^\infty C(t)(t-\tau)^2 dt}{\int_0^\infty C(t)dt} = \frac{\int_0^\infty \tau^2 \cdot C(t)dt}{\int_0^\infty C(t)dt} - \tau^2 \tag{19}$$

In equations (18) and (19), C is the measured concentration of the tracer at the outlet of the column (g/m^3) and t elapsed time from the initial injection of the tracer (sec).

Column Experiments

The transport of three bacterial strains through the porous medium of COA was evaluated using column experiments, which were conducted using a column from Kimble-Kontes (Vineland, NJ) with 2.5-cm ID × 15-cm length (T-1). COA was packed in the column through CO_2 solvation to eliminate air pockets. COA was initially saturated with 10 pore volumes of sterilized NPDI, which was introduced at the inlet of the column by a peristaltic pump

(Masterflex, Cole-Parmer, Vernon Hills, IL) at flow rates of 0.06 ml/sec and 0.1 ml/sec. A conservative pulse tracer (chloride) BTC was determined separately before the introduction of bacteria. The conductivity (μmhos) of the tracer was measured and used in equations (11) to (13) to estimate *Pe* (Fig. 1). The tracer (12 ml of 1 M NaCl) was injected via a syringe using an injection port with a pulse duration of 4 mins. For each run, 10 ml of bacterial solution (concentration predetermined by ATP analysis of 0.5 mg/ml) was injected via the syringe pump using the injection port. The column was continuously flushed with sterilized NPDI until a background ATP signal was detected from the elution collected by a fraction collector. The concentrations of ATP were then used to generate BTCs for each bacterium. For each bacterial strain at each flow rate, three runs were performed, and the inconsistency of BTCs was within 5% (95% CI). A representative BTC for each bacterium at each flow rate is illustrated in Fig. 2. After each run, mass balance was performed. Bacterial contents inside the column were measured by making the media a suspended solution to perform the ATP measurement. Relative parameters used in column experiments are listed in Table 1.

RESULTS AND DISCUSSION

CXTFIT was used to model the tracer BTCs with fixed media porosity values (27). The media porosity value was fixed since it was measured independently. The simulated velocity and *Pe* were consistent with those estimated using the method of moments, i.e., 0.057 ml/sec and 137.2 as compared to 0.06 ml/sec

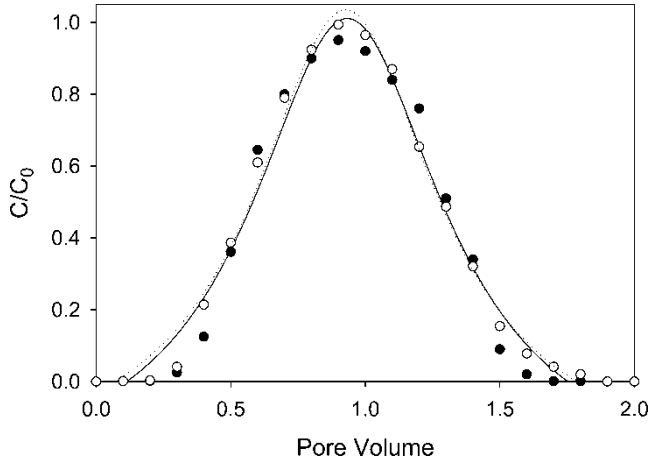

Figure 1. Tracer experiments and model simulations. Symbols are observed tracer data and lines are model simulations. Solid symbols and lines are for the flow rate of 0.06 ml/sec and hollow symbols and dotted lines are for the flow rate of 0.10 ml/sec.

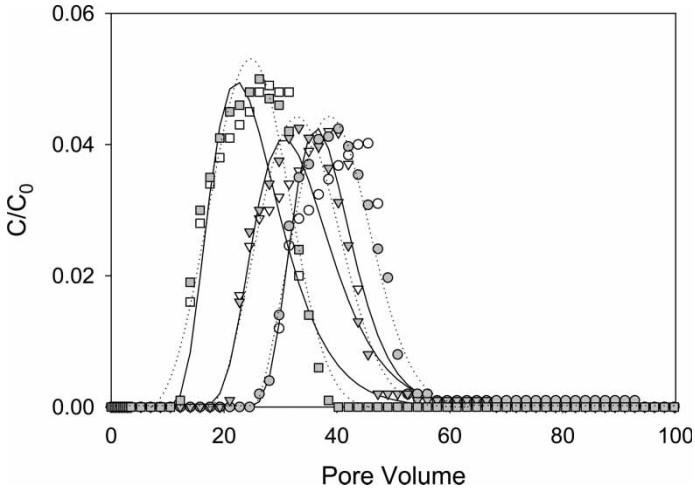

Figure 2. Microbial BTCs on COA and Model simulations. Symbols are observed microbial transport data and lines are model simulations. Solid symbols and lines are for the flow rate of 0.06 ml/sec and hollow symbols and dotted lines are for the flow rate of 0.10 ml/sec. Specifically, square symbolizes *P. sp.*; triangle symbolizes *P. putida* and circle symbolizes *P. fluorescens*.

and 152.8 for the low flow rate and 0.97 ml/sec and 246.4 as compared to 1.0 ml/sec and 254.6 for the high flow rate. Theoretically, the alluvial loam is no mono-porous medium. And yet, the alluvial loam used in this research exhibited mono surface properties, which was supported by the fact that 96% of the tracer was recovered during the experiment. All the microbial BTCs (Fig. 2) had a diffused front upon a step concentration increase and a self-sharpening front in the case of step decrease. This behavior demonstrated that the retention of the microbes on the medium increased with the increasing

Table 1. Summary of the parameters used in column experiment

Microorganisms			Diameter
P. fluorescens			~0.6 μm
P. putida			~0.6 μm
P. sp			~0.6 μm
Porous Media	Radius	Porosity	Density
COA	~65 μm	0.48	2.62 g/cm^3
Column Experiment			
Column		2.5-cm ID × 15-cm Length	
Flow Rate		0.06 ml/sec and 0.1 ml/sec	
Pe		152.8 (0.06 ml/sec) and 254.6 (0.1 ml/sec)	

concentration in solution, which led to a broad, diffused front. In the case of step decrease (desorption), the retention time decreased in time and led to the development of a narrow, self-sharpening front (11). What was more, the BTCs of the relative microbial concentration versus the pore volume of the same microbes at different pore velocities nearly superimposed (Fig. 2). Bacterial deposition has often been modeled as a first-order function. First-order bacterial deposition should be valid if bacterial attachment to porous media is rate-limiting. Recent research has discovered that multiple first-order kinetics with an uneven distribution of deposition rate coefficients may better describe bacterial attachment to the porous media. However, in this research, first order kinetics can successfully describe bacterial attachment to alluvial loam.

Bürglsser et al. (11) developed a method that allowed rapid measurements of an entire, possibly nonlinear sorption isotherm by a simple integration of the diffuse front of the BTCs. Based on this method, the concentration of reversibly adsorbed bacteria on the porous medium, S, can be obtained by integrating the experimental record of the retention time t(c) if the dispersion term in equation (3) is neglected (D = 0):

$$S = \frac{\theta}{\rho_b(1-\theta)} \int_0^c \left(\frac{t(c')}{t_0} - 1 \right) dc' - \int_0^c t(c') k_c dc' \tag{20}$$

where $t_0 = L/v$ and is the average microbial travel time in the column. The insignificant role of hydrodynamic dispersion on microbial transport has been proven by Unice and Logan (28). Schweich and Sardin (29) also demonstrated that the hydrodynamic dispersion can be neglected for $Pe > 100$. For this research, all the column experiments were performed with $Pe > 100$, thus equation (20) can be used to determine the microbial isotherms.

The microbial isotherms (Fig. 3) were obtained using equation (20) from the microbial BTCs. Since the BTCs of each bacterium at different flow rates superimposed, the isotherms were unique for each bacterium. In other words, microbial sorption isotherms were not impacted by the flow rate. All the three bacterial strains had a concave isotherm on COA. The microbial sorption isotherms can be described by the Freundlich expression:

$$S = K_{fr} C_e^N \tag{21}$$

where K_{fr} is the Freundlich partition coefficient $[(m^3/g)^N]$; N Freundlich exponent coefficient. K_{fr} and N values for the microbes are listed in Fig. 3, which were obtained using numerical simulation. It should be noted that the Freundlich isotherm is an exponential function and a small variation in N, i.e., 1.07 as compared to 1.05 makes great difference in bacterial BTCs.

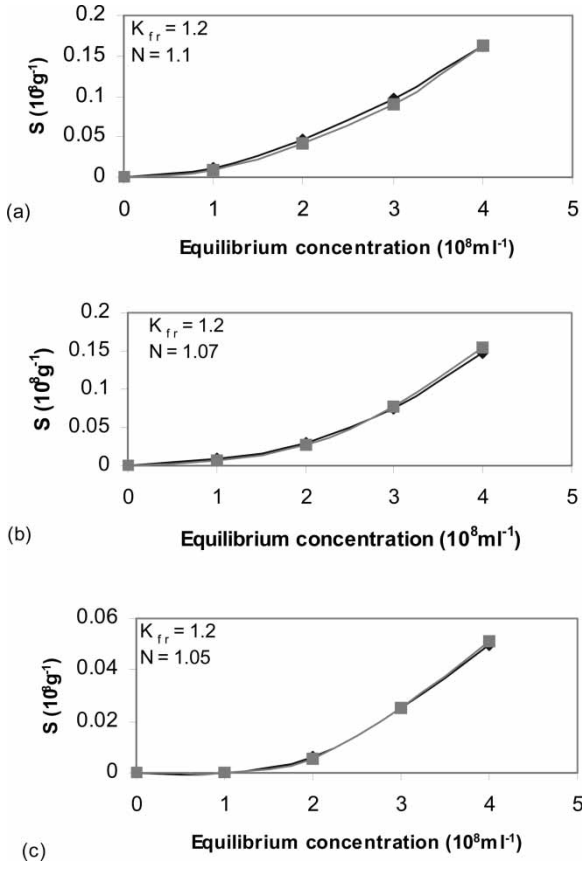

Figure 3. Microbial sorption isotherms for (a) *P. fluorescens*; (b) *P. putida*; and (c) *P.* sp.

DISCUSSION

The underlying principle behind the isotherms resulted from forms of bonding between the microbes and sorption receptor sites on the solid. The amount of sorption that occurred was dependent on the surface characteristics of the microbes and porous media. More generally, interfacial interactions between the microbes and the porous media were thought to be the driving force. To develop a surface thermodynamic explanation of the isotherms, interfacial interactions of suspended bacterial cells in the solution with the media matrices as well as with deposited cells on the media surfaces were investigated. van Loosdrecht et al. (30) and Chen and Strevett (15) discovered that microbial reversible sorption was a function of the total free energy of the interactions between bacterial cells and the media matrices at the secondary maximum.

Table 2. Bacterial and medium surface thermodynamic properties

Stain/medium	ζ-potential (mV)	γ^{LW} (mJ/m^2)	γ^+ (mJ/m^2)	γ^- (mJ/m^2)
P. fluorescens	-10.2 ± 0.1	35.4	0.42	56.9
P. putida	-10.6 ± 0.2	34.8	0.62	55.4
P. sp	-10.8 ± 0.1	34.3	0.72	53.4
COA	-42.5 ± 0.6	27.4	0.03	13.7

During the transport, deposited cells (due to irreversible sorption) on the media surfaces, cell-coating, altered the interactions between suspended bacterial cells in the solution and the media by changing the media surface properties. Based on the surface thermodynamic properties of the microbes and the media (Table 2), the interaction free energy between the microbes and the media at the secondary maximum were calculated (Table 3). As the total free energy of attractive cell-cell (between suspended and deposited bacterial cells on the media surfaces) interactions of ΔG_{131}^{TOT} at the secondary maximum (1.70 kT, 3.30 kT and 4.36 kT for *P. fluorescens*, *P. putida*, and *P.* sp. respectively) was smaller (negatively greater) than that of the cell-solid (between suspended bacterial cells and the media surfaces) interactions (85.36 kT, 89.30 kT and 91.27 kT), suspended bacterial cells in the solution had a greater potential to partition on the media surfaces covered with deposited cells. This led to an increase in bacterial reversible adsorption with the increase of microbial solution concentrations as deposited cells on the media surfaces increased accordingly. The more the media surface is covered with deposited cells, the more impact cell-cell interactions will have on the microbial reversible adsorption, which leads to concave isotherms.

Bacterial isotherms were verified in the column experiments. The microbial sorption isotherms $s = k_{fr}c_e^N$ was incorporated into equation (3)

Table 3. Interaction free energy at secondary maximum

Strain/medium	*P. fluorescens*	*P. putida*	*P.* sp
ΔG_{131}^{LW} (kT)	-7.42	-6.84	-6.37
ΔG_{131}^{AB} (kT)	-1.97	-1.83	-1.70
ΔG_{131}^{EL} (kT)	11.09	11.97	12.43
ΔG_{131}^{TOT} (kT)	1.70	3.30	4.36
ΔG_{132}^{LW} (kT)	-6.54	-6.28	-6.06
ΔG_{132}^{AB} (kT)	-0.56	-0.53	-0.48
ΔG_{132}^{EL} (kT)	92.46	96.11	97.81
ΔG_{132}^{TOT} (kT)	85.36	89.30	91.27

(assuming equilibrium was reach during the microbial transport inside the column):

$$\left(1+\frac{1-\theta}{\theta}\rho_{\mathrm{p}}\mathrm{N}\mathrm{K}_{\mathrm{fr}}\mathrm{C}^{\mathrm{N}-1}\right)\frac{\partial \mathrm{C}}{\partial \mathrm{t}}=\mathrm{D}\frac{\partial^2 \mathrm{C}}{\partial \mathrm{x}^2}-\mathrm{v}\frac{\partial \mathrm{C}}{\partial \mathrm{x}}-\mathrm{k}_{\mathrm{c}}\mathrm{C} \tag{22}$$

equation (22) was then solved using numerical methods with the following initial and boundary conditions:

$$\mathrm{C}=\mathrm{C}_0 \quad \mathrm{x}=0 \quad \text{for} \quad \mathrm{t}\le \mathrm{t}_{\mathrm{pulse}} \tag{22a}$$

$$\mathrm{C}=0 \quad \mathrm{x}=0 \quad \text{for} \quad \mathrm{t}> \mathrm{t}_{\mathrm{pulse}} \tag{22b}$$

$$\mathrm{C}=0 \quad \mathrm{x}=\mathrm{L} \quad \text{for} \quad \mathrm{t}=0 \tag{22c}$$

where C_0 is the initial injected microbial concentration. The numerical simulation was performed using an implicit, finite-difference scheme. All these parameters were optimized by minimizing the sum of squared differences between observed and fitted concentrations using the nonlinear least-square method. The simulated results were compared against experimental observations and the experimental results were successfully represented by this numerical model (Fig. 2). The fitness of the model simulation and experimental observation also confirmed that the Convection-Dispersion Model incorporated with Filtration Model to account for irreversible soprtion could be used to describe microbial transport in porous media. It should be noted that above simulation method is comparable with the method of Hendry et al. (31, 32) with different sink sources.

Theoretically, reversible sorption of the microbes on the porous medium that is determined by microbial sorption isotherms should not be impacted by the transport velocity as long as the equilibrium is reached (9); while irreversible sorption or deposition of the microbes on the porous media is greatly impacted by the transport velocity through its impact on retention time (2). This was also validated in this study. The same bacterial strain had the same sorption isotherms but different deposition coefficient at different flow rates (4.64 hr^{-1}, 4.39 hr^{-1} and 4.17 hr^{-1} for *P. fluorescens*, *P. putida*, and *P.* sp. at a flow rate of 0.06 ml/sec respectively and 7.74 hr^{-1}, 7.33 hr^{-1} and 6.96 hr^{-1} at a flow rate of 0.1 ml/sec). To investigate the reason that the BTCs of the same microbes at different flow rates nearly superimposed, equation (20) is rearranged to incorporate equation (16) and the concentration dependent retention time is expressed in term of microbial sorption isotherms and fraction recovery (obtained by integration of the BTCs):

$$\frac{t(c')}{t_0}=\frac{\dfrac{\rho_b(1-\theta)}{\theta}\dfrac{dS}{dC}+1}{1+Ln(fr)-\dfrac{Ln^2(fr)}{Pe}} \tag{23}$$

In equation (23), the term $\mathrm{Ln}^2(\mathrm{fr})/\mathrm{Pe}$ can be neglected for $\mathrm{Pe} > 100$ due to the insignificant role of hydrodynamic dispersion on microbial transport under

conditions of this research (28, 29). Microbial isotherms (dS/dC) is not impacted by the flow rate (9), neither is the fraction recovery (fr) (15). Based on equation (23), as the term $Ln^2(fr)/Pe$ was neglected in this research ($Pe = 152.8$ for the flow rate of 0.06 ml/sec and $Pe = 254.6$ for 0.1 ml/sec), the concentration dependent retention time was independent of transport velocity, which made the BTCs of the same microbes nearly superimposed at different flow rates. It should also be noted that for conditions where $Pe < 100$, or hydrodynamic dispersion cannot be ignored, the BTCs will be different for different flow rates.

CONCLUSION

The main achievement of this study is to provide a way of determination of microbial adsorption isotherms using column experiments, which cannot be achieved using the traditional batch methods due to the difficulty of distinguishing between reversible and irreversible sorption. A further advantage of the column methods is that a high solid to solution ratio close to that is encountered in the natural systems is used for the determination of microbial sorption isotherms, which is more practically reliable. Also, a surface thermodynamic explanation of the concave-shaped microbial sorption isotherms was also reached in this study and the impact of transport velocity on the microbial BTCs was discussed. This study will be of great importance in understanding the fate and transport of microbes in the subsurface, and will provide useful guidance for *in-situ* bioremediation. Further tests will be performed in the future to make the above discussed equations applicable for prediction.

REFERENCES

1. Fontes, D.E., Mills, A.L., Hornberger, G.M., and Herman, J.S. (1991) Physical and chemical factors influencing transport of microorganisms through porous media. *Appl. Environ. Microbiol.*, 57 (9): 2473–2481.
2. Bolster, C.H., Hornberger, G.M., Mills, A.L., and Wilson, J.L. (1998) A method for calculating bacterial deposition coefficients using the fraction of bacteria recovered from laboratory columns. *Environ. Sci. Technol.*, 32 (9): 1329–1332.
3. Powelson, D.K. and Mills, A.L. (1998) Water saturation and surfactant effects on bacterial transport in sand columns. *Soil Sci.*, 163 (9): 694–704.
4. Gamerdinger, A.P., van Rees, K.C.J., Rao, P.S.C., and Jessup, R.E. (1994) Evaluation of *in situ* columns for characterizing organic contaminant sorption during transport. *Environ. Sci. Technol.*, 28 (3): 376–382.
5. Hornberger, G.M., Mills, A.L., and Herman, J.S. (1992) Bacterial transport in porous media: evaluation of a model using laboratory observations. *Water Resour. Res.*, 28 (3): 915–938.
6. Harvey, R.W. and Garabedian, S.P. (1991) Use of colloid filtration theory in modeling movement of bacteria through a contaminated sandy aquifer. *Environ. Sci. Technol.*, 25 (1): 178–185.

7. Gannon, J.T., Mingelgrin, U., Alexander, M., and Wagenet, R.J. (1991) Bacterial transport through homogeneous. *Soil Biol. Biochem.*, 23 (12): 1155–1160.
8. Elimelech, M. and O′Melia, C.R. (1990) Kinetic of deposition of colloidal particles in porous media. *Environ. Sci. Technol.*, 24 (10): 1528–1536.
9. Dohse, D.M. and Lion, L.W. (1994) Effect of microbial polymers on the sorption and transport of phenanthrene in a low-carbon sand. *Environ. Sci. Technol.*, 28 (4): 541–548.
10. Bellin, C.A. and Rao, P.S.C. (1993) Impact of bacterial biomass on contaminant sorption and transport in subsurface soil. *Appl. Environ. Microbiol.*, 59 (6): 1813–1820.
11. Bürgisser, C.S., Černík, M., Borkovec, M., and Sticher, H. (1992) Determination of nonlinear adsorption isotherms from column experiments: an alternative to batch studies. *Environ. Sci. Technol.*, 27 (5): 943–948.
12. Jenkins, M.B. and Lion, L.W. (1993) Mobile bacteria and transport of polynuclear aromatic hydrocarbons in porous media. *Appl. Environ. Microbiol.*, 59 (10): 3306–3313.
13. Magee, B.R., Lion, L.W., and Lemley, A.T. (1991) Transport of dissolved organic macromolecules and their effect on the transport of phenanthrene in porous media. *Environ. Sci. Technol.*, 25 (2): 323–331.
14. Nkedi-Kizza, P., Rao, P.S.C., and Hornsby, A.G. (1987) Influence of organic cosolvents on leaching of hydrophobic organic chemicals through soils. *Environ. Sci. Technol.*, 21 (11): 1107–1111.
15. Chen, G. and Strevett, K.A. (2002) Surface free energy relationships used to evaluate microbial transport. *J. Environ. Eng.*, 128 (5): 1–8.
16. Knox, R.C., Sabatini, D.A., and Canter, L.W. (1993) *Subsurface Transport and Fate Processes*; Lewis Publishers: New York.
17. Hancock, I. and Poxton, I. (1988) *Bacterial Cell Surface Techniques*; John Wiley & Sons: New York.
18. Karapanagioti, H.K., Kleineidam, S., Ligouis, B., Sabatini, D.A., and Grathwohl, P. (1999) Phenanthrene sorption with heterogeneous organic matter in a landfill aquifer material. *Phys. Chem. Earth.*, 24 (6): 535–541.
19. Wålinder, M.E. and Gardner, D.J. (1999) Factors influencing contact angle measurements on wood particles by column wicking. *J. Adhesion Sci. Technol.*, 13 (12): 1363–1374.
20. Ku, C. and Henry, J.D., Jr. (1985) Mechanisms of particle transfer from a continuous oil to a dispersed water phase. *J. Colloid Interface Sci.*, 116 (2): 414–422.
21. Grasso, D., Smets, B.F., Strevett, K.A., Machinist, B.D., van Oss, C.J., Giese, R.F., and Wu, W. (1996) Impact of physiological state on surface thermodynamics and adhesion of *Pseudomonas aeruginosa*. *Environ. Sci. Technol.*, 30 (12): 3604–3608.
22. Meinders, J.M., van der Mei, H.C., and Bussher, H.J. (1995) Deposition efficiency and reversibility of bacterial adhesion under flow. *J. Colloid Interface. Sci.*, 176 (2): 329–341.
23. van oss, C.J. (1994) *Interfacial Forces in Aqueous Media*; Marcel Dekker: New York.
24. Marshall, K.C., Breznak, J.A., Calleja, G.B., Mcfeters, G.A., and Rutter, P.R. (1984) *Microbial Adhesion and Aggregation*; Springer-Verlag: New York.
25. Annable, M.D., Rao, P.S.C., Hatfield, K., Graham, W.D., Wood, A.L., and Enfield, C.G. (1998) Partitioning tracers for measuring residual NAPL: field-scale test results. *J. Environ. Eng.*, 124 (6): 498–503.

26. Jin, M., Delshad, M., Dwarakanath, V., McKinney, D.C., Pope, G.A., Sepehrnoori, K., Tiburg, C., and Jackson, R.E. (1995) Partitioning tracer test for detection, estimation, and remediation performance assessment of subsurface phase liquid. *Water Resour. Res.*, 31 (5): 1201–1211.
27. Toride, N., Leij, F.J., and van Genuchten, M.T. (1995) The CXTFIT Code for Estimating Transport Parameters from Laboratory or Field Experiments, Version 2.1, Research Report 137. U.S. Salinity Laboratory, Riverside, CA.
28. Unice, K.M. and Logan, B.E. (2000) Insignificant role of hydrodynamic dispersion of bacterial transport. *J. Environ. Eng.*, 126 (6): 491–500.
29. Schweich, D. and Sardin, M. (1981) Adsorption, partition, ion exchange and chemical reaction in batch reactors or in columns—a review. *J. Hydrol.*, 50 (1): 1–33.
30. van Loosdrecht, M.C.M., Lyklema, J., Norde, W., and Zehnder, A.J.B. (1989) Bacterial adhesion: a physicochemical approach. *Microb. Ecol.*, 17 (1): 1–15.
31. Hendry, M.J., Lawrence, J.R., and Maloszewski, P. (1999) Effects of velocity on the transport of two bacteria through saturated sand. *Ground Water*, 37 (1): 103–112.
32. Hendry, M.J., Lawrence, J.R., and Maloszewski, P. (1997) The role of sorption in the transport of Klebsiella oxytoca through saturated silica sand. *Ground Water*, 35 (4): 574–584.